Harmonic and Power Loss Minimization in Power Systems Incorporating Renewable Energy Sources and Locational Marginal Pricing

Saheed Lekan Gbadamosi*, Nnamdi I. Nwulu, Y. Sun

Department of Electrical and Electronic Engineering Science, University of Johannesburg, Auckland Park 2006, South Africa

* Corresponding author email: gbadamosiadeolu@gmail.com

ABSTRACT

In composite expansion planning, improving the efficiency and power quality of power supplied from Renewable Energy Sources (RES) is highly essential. Therefore, this paper focuses on developing an optimal power flow optimization model for minimizing power loss and harmonics emanating from RES with emphasis on reducing their impacts on the Locational Marginal Prices (LMP). In order to assess the magnitude of harmonics, grid modelling and simulation with RES such as wind and solar energy was carried out using the Electrical Transient Analyzer Program (ETAP 12.6.0) software. The proposed mixed integer nonlinear programming mathematical model was solved using the Outer Approximation Algorithm (AOA) solver in the Advanced Interactive Multidimensional Modelling System (AIMMS), and the efficiency of the model was tested on the modified IEEE 6 bus and 24 bus system. The results obtained from simulations reveal the efficiency of the proposed model in terms of effective costs reduction, nodal marginal price reduction, minimization of harmonic losses and additional lines in the power system network.

Keywords: Expansion planning, Harmonics, Locational marginal price, Optimization, Renewable energy sources.

Nomenclature

Sets

n_b number of buses

n_h number of order of harmonics

n_i number of conventional generators

n_k number of loads

n_{cl} number of candidate lines

n_{el} number of existing lines

n_l number of transmission lines

n_s number of prospective solar pv generators

n_w number of prospective wind generators

Indices

b bus

h harmonic order

i conventional generating unit

k load

cl candidate transmission line

el existing transmission line

l transmission line

q generation option of prospective generating unit

α sending end bus

β receiving end bus

p nodal price

s prospective solar pv generating unit

w prospective wind generating unit

Parameters

b_l and b_{lo} susceptance and shunt susceptance of transmission line l (ohms).

C_i generation cost of conventional generating unit i ($/MWh)

$P_i^{\min}$ and $Q_i^{\min}$ minimum generating capacity of real and reactive power of generating unit i (MW and MVAr).

$P_i^{\max}$ and $Q_i^{\max}$ maximum generating capacity of real and reactive power of generating unit i (MW and MVAr).

$\overline{P_w}$ and $\overline{P_s}$ maximum bound of generation capacity investment of prospective wind and solar pv generating unit w and s respectively (MW).

P_k and Q_k real and reactive power of load k (MW)

$V_{\min}$ and $V_{\max}$ minimum and maximum magnitude of voltage at bus b (p.u).

R_l and g_l resistance and conductance of transmission line l (ohms)

P_{wq} and P_{sq} generation capacity of investment choice q of prospective wind and solar pv generating unit w and s respectively.

I_w and I_s annualized investment cost of prospective wind and solar pv generating unit w and s respectively ($/MW).

I_{cl} annualized investment cost of candidate transmission line cl ($).

V_α and V_β sending and receiving end bus respectively (p.u).

V_b^h voltage magnitude of harmonic order h in bus b (%).

Z_l^h impedance for harmonic order h in line l (ohms)

Y_n^h admittance for harmonic order h in bus b (ohms)

Y_l^h admittance for harmonic order h in line l (ohms)

Ω_w and Ω_s investment budget for prospective wind and solar pv generating unit w and s respectively ($).

Ω_{cl} investment budget for candidate line cl ($).

N_p nodal price p of the network without RES ($/MW)

$N_{RES,p}$ nodal price p with incorporation of RES ($/MW)

∂ duration of operation (h)

$IHD_V^{\max}$ and $THD_V^{\max}$ maximum individual harmonic distortion and total harmonic distortion of voltage respectively (%).

$\sigma_1, \sigma_2, \sigma_3, \sigma_4$ and σ_5 weight factor for objective function.

a_i, b_i and c_i generation cost coefficients of conventional generating unit i.

s_i, t_i and u_i emission coefficients of conventional generating unit i.

x_p, y_p and z_p nodal price coefficients as a function of harmonics.

Variables

P_i and Q_i real and reactive power capacity of conventional generating unit i (MWh and MVArh).

P_w and Q_w real and reactive power capacity of prospective wind generating unit w (MW and MVAr).

P_s and Q_s real and reactive power capacity of prospective solar generating unit s (MW and MVAr).

P_w^{max} and P_s^{max} capacity of prospective wind and solar pv generating unit w and s respectively (MW).

η_{wq} and η_{sq} binary decision variable generating option q of prospective wind and solar pv generating unit w and s respectively.

η_{cl} binary decision variable that is 1 if candidate transmission line l is built and 0 otherwise.

P_{Loss} and Q_{Loss} real and reactive power loss on the transmission line l (MW and MVAr).

$F_l^{(outflow)}$ and $Q_l^{(outflow)}$ real and reactive outflowing power capacity from the sending end bus (MW and MVAr).

$F_l^{(inflow)}$ and $Q_l^{(inflow)}$ real and reactive inflowing power capacity to the receiving end bus (MW and MVAr).

$N_{RES,p}^h$ nodal price p as a function of harmonic order h ($/MW)

μ_b^h active power loss for harmonics order h on bus b (MW).

μ_l^h active power loss for harmonics order h on transmission line l (MW).

I_l^h magnitude of current harmonic order h on transmission line l.

I_b^h magnitude of current harmonic order h on bus b.

$\theta_{\alpha\beta}$ voltage angle between the sending end (α) and receiving end (β) bus.

V_b voltage magnitude on bus b (p.u).

I. INTRODUCTION

The uncertainties associated with fossil fuel prices and ability of ensuring long time energy security has boosted the consistent growth of renewable energy technologies in the world. Renewable Energy Sources (RES) play an impressive role in electricity generation resulting in sustainable worldwide electrification. Wind and solar energy are the cheapest, widely available sources of renewable energy and also possess unique benefits such as lack of harmful emissions, increased energy efficiency etc. Their potentials to reduce heavy dependence on fossil fuels whilst ensuring energy efficiency and also meeting the ever-increasing energy demand, places them as a key factor in energy transition.

The current technological evolution in renewable energy technologies especially with respect to wind energy compels the energy supply to come from a significant distance (typically offshore) due to the accessibility of higher wind speeds resulting in increased generation capacity. Integrating the offshore power into the grid has adverse impacts on the power quality of electric power system, which is a big challenge for network planners in the energy sector. Due to prevailing challenges that comes with penetration of large renewable energy into the grid, researchers in academia and industries are focusing on the negative influence of harmonics on the power system network. The renewable energy sources exhibit some features that make it a source of harmonic to the grid due to the interactions between wind turbines and the new transmission medium linking offshore to onshore. High Voltage Direct Current (HVDC) technology has recently been used to connect a large number of offshore wind power to grid. The increasing use of this kind of power electronic device produces waveform distortion in the output power, generating harmonics with adverse effects such as voltage and current distortions, electromagnetic interferences, low power factor and low efficiency [1].

More importantly, both wind turbines and large scale solar farms employs the inverters for power conversion, the output of this power electronic inverters contains a substantial proportion of harmonics which have harmful effects on the mechanical and electrical system components [2]. The presence of harmonics in the RES and HVDC transmitting medium may result in the possibility of exceeding the maximum permissible values for individual and total harmonic distortion of voltage and currents as specified by the IEEE standard 519 [3], and, harmonic distortion above the limits can lead to mis-operation of relays, circuit breaker, electric meters, premature aging of electrical components and even complete collapse of renewable energy generation plant [4][5]. Also, it can result into electrical energy losses in the network and in turn increase the cost of electricity generation and network operational costs. Presently, harmonic distortions do not have economic value but there exist significant financial consequences to the negative impacts it contributes to the power system. The economic losses can be connected to the negative influence of harmonics on the power system equipment resulting into higher maintenance costs for aging equipment and decrease in accuracy of the meter that can alter electricity market transactions [6] [7].

Recently, a few works discussed the impacts of harmonics on the power system network. Reference [8] discussed the issues related to harmonics as regards power quality and distribution

system planning with Distributed Energy Resource (DERs). A new Modified Group experience of Teaching Learning Based Optimization (TLBO) approach was proposed for optimal allocation of DERs and as well as minimizing the losses whilst retaining the magnitude of harmonic distortion at their standard limits. Reference [9] presents a Generalized Harmonic Distribution Factor method to earmark the transmission loss cost as a result of harmonics on the network, however, the authors did not consider harmonic emission from the power sources but only those emitting from nonlinear loads. Reference [6] discussed harmonic emissions from multiple DER sources and energy storage systems that can affect distribution network system and the authors proposed an index of phasor harmonics (IPH) for analyzing harmonics and as well as considering magnitude and angle of waveform using data visualization approach. In [10] the authors developed an optimization process for electrical network expansion by examining the platform that minimizes the power quality in the electrical system and they only considered minimizing the voltage sag. In [11], the authors studied behavior of harmonics emission in a wind farm. The analysis of random behavior of harmonic emissions are done from experimental measurements. The authors proposed two probability distribution functions to characterize the uncertain behavior of the harmonic current. Reference [12] developed an approach for harmonic studies of a doubly fed induction generator and a full power converter fed generator. IPSA simulation package was used to model the turbine generator and the components of the wind farm so as to assess the harmonics at the connection point. It was concluded that the long transmission cables impedance dominates the harmonic impedance which is characterized by series of resonances. References [8]- [14] confirmed the emission of harmonics from nonlinear loads and RES, but the level of their distortions and the magnitudes of their impact on expansion planning were not considered.

Power system expansion planning plays a critical role in the restructuring of the power industry by providing an enabling environment for its participants[15]. The system planner needs to perfectly determine the costs associated with the integration of new renewable energy sources, thereby creating price indications that reflect the time and location value of electricity [16] [17]. Typically, locational marginal prices (LMP) are commonly used in market-based techniques. Locational marginal price is referred to as the marginal cost of generation and transmission to serve an additional megawatt (MW) of load at a given location. LMP must ensure adequate evaluation of harmonic distortion quantities present by effective allocation of harmonic voltages and currents at each node of the system network. Therefore, marginal pricing at one location must vary from another due to the impact of harmonics variation in the transmission lines.

Some publications present some works that considered the impact of power losses on locational marginal prices as well as impacts of LMP on wind generation. Reference[18] minimized power loss of the system using loss sensitivity factor to predetermine the capacitor optimal location. Reference [19] developed locational marginal pricing model as an optimization problem with the intention of mitigating losses on the network. The presented LMP policy determines the DG units which are involved in reduction of losses and encouraged to increase generation due to the rise in the LMP of DG units. Reference [20] presented a modelling framework to limit revenue or cost changes for generation and load during the transition of

financial transmission rights from uniform to nodal pricing. Reference [21] used of artificial neural network (ANN) technique for forecasting wind power and LMP, and an energy storage system (ESS) was utilized when LMP is unstable due to wind deficiency. The authors also proposed a stochastic locational marginal price energy market model incorporating power generated from wind at different locations of the system and investigated the impacts of wind farm capacity during wake effect on the LMP market. Reference [22] discussed wind production impacts on the locational marginal prices using DC model. The wind power was modelled as negative loads in the electricity market. Results showed changes in LMP average values with respect to the increase in wind power penetration, but the authors did not consider the impacts of harmonics from wind power plant on LMP. Authors of [23], evaluated the locational marginal prices with real and reactive power at each bus using AC optimal power flow. The operational cost of reactive power for both the generators and reactive compensators was incorporated into the objective function. The OPF problem was solved using the combination of interior point method and branch and bound method. In [24], the author presented a network constrained economic dispatch based on DC model to explore the locational impacts of slack bus on LMP using transmission loss factor (TLF) in the commercialized electricity industries. Reference [25] used of nodal pricing to locate DG resources in distribution network and the results showed that DG resource has substantial more revenue reflecting its contribution in mitigating line losses and loading. All the literatures mentioned above offer valuable contributions, but no reference describes the effect of harmonic losses on composite expansion planning of a power with RES. There exists no mathematical model or formulation to quantify the associated influence of this losses on the expansion planning system. In this paper, the impacts of harmonic and power losses from offshore wind and solar farms together with static converters of the HVDC transmitting medium on the locational marginal pricing and generation dispatch on the power system network is investigated.

A new mathematical formulation is presented to minimize costs, nodal marginal prices, active power losses and harmonic losses in the network. The main contributions of the proposed model are listed below:

- achieving a new method of calculating optimal locational marginal price as a function of harmonic power loss from RES.
- developing an approach for effective minimization of costs and losses associated with RES integration.
- application of regression analysis for obtaining nodal marginal price coefficients at the buses.
- evaluation of harmonics influences on generation and transmission expansion planning system.

The paper is organized as follows: In Section II, the harmonics model of RES components is presented; Section III presents the problem formulation; in Section IV, the proposed model is implemented using two case studies; Section V presents the simulation results and discussion of results and the study is concluded in Section VI.

II. HARMONIC MODELS FOR RENEWABLE ENERGY SOURCE COMPONENTS

The objective of this study is to evaluate harmonic magnitudes from offshore RES (wind and solar farms) and HVDC transmitting medium. In this paper, harmonic can affect power system network is via three harmonic sources as outlined below:

- The nonlinear behaviour of the wind turbines.
- The operation of modern power electronic switches such as MOSFETs and IGBTs, which are present in the PV inverter [26].
- The topology structure and switching control strategy of HVDC converter valves, which represent a nonlinear impedance to the generating systems.

Hence, the harmonic studies are required to quantify the magnitude of harmonic emissions from harmonic sources at the point of common coupling (PCC).

A. Offshore wind farm and solar PV farm modelling

In order to analyze the flow of harmonics in the network, proper harmonic source modeling is essential. The main aim of simulation is to investigate the harmonic current emissions of power electronic-based generators as shown in Fig.1. In this paper, the simulation model of offshore wind and solar farm is developed in Electrical Transient Analyzer Program (ETAP 12.6.0) software.
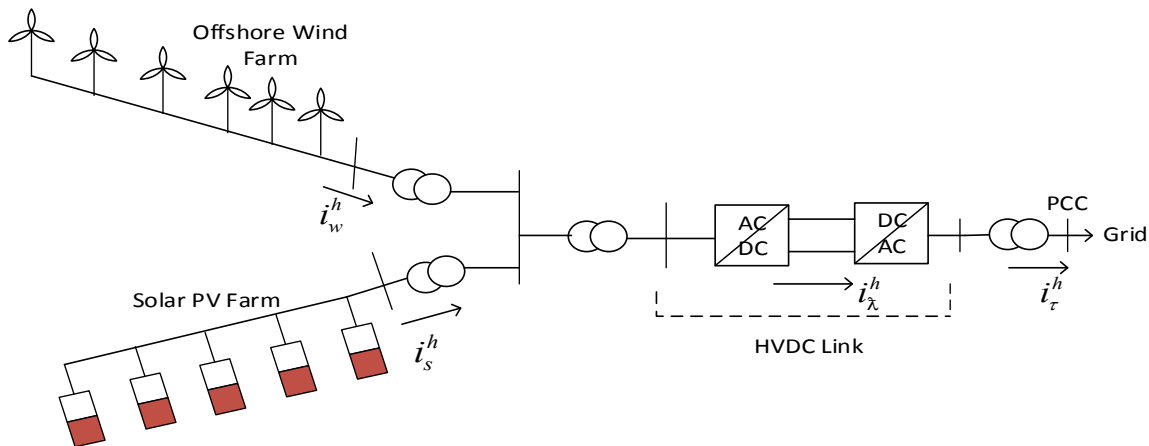

Figure 1: One Line Diagram of Harmonic Current Flow in Offshore Wind and PV Farms.

The current harmonics obtained at the point of common coupling (PCC) depends on the sum of individual wind turbine harmonic currents, sum of individual solar PV harmonic currents and the sum of individual HVDC static converter harmonic currents, which is given as:

$$\sum_{w=1}^{n_w} i_w^h + \sum_{s=1}^{n_s} i_s^h + \sum_{\lambda=1}^{n_\lambda} i_\lambda^h = i_\tau^h \tag{1}$$

where i_w^h represents the individual wind farm harmonic currents, i_s^h represents individual solar farm harmonic currents, i_λ^h represents individual HVDC converter harmonic currents and i_τ^h represent the individual harmonic currents obtained at the PCC. The harmonic currents obtained at PCC display some kinds of stochastic behaviors, such that the magnitude of the total harmonic emissions is less than the sum of the magnitudes of harmonic emissions from different contributions. This is because variations in harmonic emission do not occur at the same time for the individual harmonic sources and this effect is referred to as harmonic aggregation. The harmonic aggregation at certain harmonic order diverges between different harmonic contributions or locations and this is described according to the standard summation rule of harmonic currents [27]:

$$I^h = \sqrt[\varepsilon]{\sum_{\tau=1}^{M} (i_\tau^h)^\varepsilon} \qquad \left(\begin{array}{ll} \varepsilon = 1 & h < 5 \\ \varepsilon = 1.4 & 5 \le h \le 10 \\ \varepsilon = 2 & 10 < h \le 999 \end{array} \right) \tag{2}$$

where I^h represents the aggregation of harmonic currents, M represents the number of harmonic sources and ε is the aggregation component.

B. Line parameter's modelling

Transmission lines have a tendency of magnifying harmonic voltages from renewable energy sources due to the presence of huge capacitance of the long transmission lines. The combination of these capacitances and line inductances give rise to network resonances. The alignment of frequencies of network resonances with the harmonics from renewable energy sources result into amplification of harmonic frequencies, which can lead to various malfunctions and failure of power system components as stated earlier. The resultant harmonic line impedance is modeled as described below [28]:

$$Z_l^h = R_l + jhX_l \tag{3}$$

Inverting the network harmonic line impedance (Z_l^h) yields the harmonic admittance matrix. Hence for each order of harmonics, admittance will be generated separately and the resultant harmonic line admittance (Y_l^h) is given as:

$$Y_l^h = \frac{1}{Z_l^h} \tag{4}$$

where R_l and X_l are the line resistance and reactance respectively; and h represent the number of harmonic order.

III. MATHEMATICAL MODEL

This section describes the mathematical model that minimizes the total costs, transmission losses, harmonic losses and locational marginal prices in a composite expansion planning model. The problem formulation is deterministic. The novelty in the proposed optimization model can be found in: (i) harmonic power loss in the objective function; (ii) locational marginal prices with respect to harmonics given in Equations (5)-(7); (iii) harmonic constraints given in equations (10)-(15); (iv) budgetary constraints for prospective lines and generators; (v) prospective optimal generating capacity limits for wind and solar farms given in equations (19)-(24).

A. Objective Functions

The proposed multi-objectives mathematical optimization model is a deterministic mixed integer nonlinear programming (MINLP). In this paper, the multi-objectives models developed focus on:

(i) economic objectives which are total costs (investment and operational costs) and nodal marginal prices given in equations (5) and (6);

(ii) technical objectives which includes active power loss and harmonic power loss as given in equations (7) and (8).

The multi-objectives functions in the network are formulated as follows:

$$Min\sigma_1 \left(\sum_{w=1}^{n_w} I_w P_w^{max} + \sum_{s=1}^{n_s} I_s P_s^{max} + \sum_{l \in cl}^{n_{cl}} I_{cl} \eta_{cl} + \partial \sum_{i=1}^{n_i} C_i(P_i) \right) \tag{5}$$

$$Min\sigma_2 \left(\sum_{b=1}^{n_b} N_{RES,p}^h(\mu_b^h) \right) \tag{6}$$

$$Min\sigma_3 \left(V_\alpha^2 + V_\beta^2 - 2V_\alpha V_\beta \cos\theta_{\alpha\beta} \right) \tag{7}$$

$$Min\sigma_3 \left(\sum_{l=1}^{n_l} \sum_{h=2}^{n_h} I_l^2 R_l \right) \tag{8}$$

The nodal marginal price Equations (9) and (10)) thus represent the quadratic function that present the relationship between the nodal marginal price and harmonic power loss. The marginal price coefficients are obtained from the simulated individual harmonic distortions using Waikato Environment for Knowledge Analysis (WEKA) software. Equation (11) presents the operational fuel costs of the conventional generating units in \$/h as a function of its output power and likewise

$$N_{RES,p} = f(\mu_b^h) \tag{9}$$

$$N_{RES,p}^h = x_p + y_p \mu_b^h + z_p(\mu_b^h)^2 \tag{10}$$

$$C_i(P_i) = a_i + b_i P_i + c_i P_i^2 \tag{11}$$

B. Model Constraints

The objective functions (6)-(9) is subject to the following constraints:

- Harmonic power flow balance

The harmonic power flow equations are given by Equation (12), which is reflected as the product of the admittance matrix and voltage harmonics at each bus. The admittance matrix will be generated separately for each harmonic order h.

$$I_b^h = V_b^h Y_b^h; \forall b = 1, 2, ..., n_b, \forall h = 2, 3, ..., n_h \tag{12}$$

- Limit on harmonic power loss at the buses

Harmonic current phase angle may not necessarily be required for studying harmonic current flow as shown in Fig. 1, but they are crucial for analyzing harmonic power loss at the bus. For harmonic sources connected at these buses, magnitudes and phase angles of the harmonics are characterized by their random behaviors. Hence, the harmonic power loss constraint reflects the magnitudes of harmonic current and voltage, together with harmonic phase angles between them and this is given in the constraint (13):

$$\mu_b^h = V_b^h I_b^h \cos\theta_{\alpha\beta} \forall b = 1, 2, ..., n_b, \forall h = 2, 3, ..., n_h \tag{13}$$

- Limit on harmonic current on the transmission line

Harmonic currents produced by renewable energy sources are amplified by the resonance which increase the magnitude of harmonics present on the line. The harmonic voltage between the sending and receiving buses, and the calculated harmonic admittance amplified the harmonic current flowing on the transmission line as given in the constraint (14).

$$I_l^h = \left| V_\alpha^h - V_\beta^h \right| Y_l^h \forall l = 1, 2, ..., n_l, \forall h = 2, 3, ..., n_h \tag{14}$$

- Limit on harmonic power flow on the transmission line

The analysis of harmonic power flow on transmission line is usually performed to ascertain the magnitude of resonant conditions that exist on the lines. The harmonic power flow equation, mathematically reflects the variation in magnitude of harmonic currents and voltages on the line as expressed in the constraint (15):

$$\mu_l^h = V_l^h I_l^h \forall l = 1, 2, ..., n_l, \forall h = 2, 3, ..., n_h \tag{15}$$

- Limit on voltage total harmonic distortion

Harmonic voltage is a serious issue in power quality, which affects all the loads connected to the point of common coupling on the network. Total harmonic distortion is an index that is widely used to determine the quantity of harmonic distortions on the network buses. This is defined as

ratio of individual harmonics and fundamental harmonics of either the voltage and current and is given as in the constraint (16). Therefore, the total harmonic distortion at the buses must not exceed the recommended limit as specified by IEEE 519 [9].

$$THD_V \leq THD_V^{\max} \, \forall h = 2,3,...,n_h \tag{16}$$

- Limit on individual harmonic distortion for voltage

Individual harmonics emission by harmonic sources must be within in acceptable limit as expressed by the grid operators. Constraint (17) gives an expression for individual harmonic distortion.

$$V^h \leq IHD_V^{\max} \, \forall h = 2,3,...,n_h \tag{17}$$

- Limit on budgetary for prospective lines

The budget constraint for transmission line expansion are taken into consideration during the expansion planning by the system operators. Hence, constraint (18) ensures that total cost of constructing candidate lines is less than or equal to the available budget for transmission lines.

$$\sum_{l \in cl}^{n_{cl}} I_{cl} \eta_{cl} \leq \Omega_{cl} \, \forall cl = 39,40,...,n_{cl} \tag{18}$$

- Limit on budgetary for prospective wind and solar generating units

The budget constraint for generation expansion planning is considered, this constraint indicates the maximum boundary on total spending by the system planners. Also, to further reduce generation costs, the system planner may adopt the large investment budget for renewable energy expansion. Therefore, constraints (19) and (20) impose investment budgets for construction of prospective offshore wind and solar generating units.

$$\sum_{w=1}^{n_w} I_w P_w^{\max} = \Omega_w \, \forall w = 1,2,...,n_w \tag{19}$$

$$\sum_{s=1}^{n_s} I_s P_s^{\max} = \Omega_s \, \forall s = 1,2,...,n_s \tag{20}$$

- Limit on generation capacity for wind generating units

Constraint (21) enforce limits on the generating capacity of each prospective offshore wind generating unit to be built.

$$0 \leq P_w^{\max} \leq \overline{P_w} \, \forall w = 1,2,...,n_w \tag{21}$$

Constraint (22) limits the capacity of each prospective offshore wind generating unit built over the planning period.

$$P_w^{\max} = \sum_q \eta_{wq} P_{wq} \; \forall w = 1, 2, ..., n_w \tag{22}$$

Constraint (23) enforce that a prospective offshore wind generating unit can only be built once.

$$\sum_q \eta_{wq} = 1 \forall w = 1, 2, ..., n_w \tag{23}$$

- Limit on generation capacity for solar generating units

Constraint (24) enforce limits on the generating capacity of each prospective offshore solar generating unit to be built.

$$0 \le P_s^{\max} \le \overline{P_s} \forall s = 1, 2, ..., n_s \tag{24}$$

Constraint (25) limit the capacity of each prospective offshore wind generating unit built over the planning period.

$$P_s^{\max} = \sum_q \eta_{sq} P_{sq} \; \forall s = 1, 2, ..., n_s \tag{25}$$

Constraint (26) enforce that a prospective offshore wind generating unit can only be built once.

$$\sum_q \eta_{sq} = 1 \forall s = 1, 2, ..., n_s \tag{26}$$

- Power balance limit

In the network, the real and reactive power balance constraints in (27) and (28) ensures that at any bus b, the total power generated by conventional generating units i, by prospective wind generating units w, by solar generating units s, minus the sum of inflowing power and outflowing power in the transmission lines equals the demand k.

$$\sum_i^{n_i} P_i + \sum_w^{n_w} P_w + \sum_s^{n_s} P_s - \sum_{l \in sl}^{n_l} F_l^{(outflow)} + \sum_{l \in rl}^{n_l} F_l^{(inflow)} = \sum_k^{n_k} P_k \forall b = 1, 2, ..., n_b \tag{27}$$

$$\sum_i^{n_i} Q_i + \sum_w^{n_w} Q_w + \sum_s^{n_s} Q_s - \sum_{l \in sl}^{n_l} Q_l^{(outflow)} + \sum_{l \in rl}^{n_l} Q_l^{(inflow)} = \sum_k^{n_k} Q_k \forall b = 1, 2, ..., n_b \tag{28}$$

- Limit on power flow on the transmission line

The mathematical equation of power flow is an expression of the change in bus voltages and transmission line parameters. The real and reactive outflowing and inflowing power on the transmission lines can be calculated using constraints (29) to (32) respectively.

$$F_l^{(outflow)} = V_\alpha g_l - V_\alpha V_\beta (g_l \cos \theta_{\alpha\beta} + b_l \sin \theta_{\alpha\beta}) \forall l = 1, 2, ..., n_l \tag{29}$$

$$Q_l^{(outflow)} = -V_\alpha (b_l + b_{lo}) + V_\alpha V_\beta (g_l \cos \theta_{\alpha\beta} - b_l \sin \theta_{\alpha\beta}) \forall l = 1, 2, ..., n_l \tag{30}$$

13

$$F_l^{(inflow)} = V_\beta g_l - V_\alpha V_\beta (g_l \cos \theta_{\alpha\beta} \text{-} b_l \sin \theta_{\alpha\beta}) \forall l = 1, 2, ..., n_l \tag{31}$$

$$Q_l^{(inflow)} = -V_\beta (b_l \text{+} b_{lo}) + V_\alpha V_\beta (b_l \cos \theta_{\alpha\beta} \text{+} g_l \sin \theta_{\alpha\beta}) \forall l = 1, 2, ..., n_l \tag{32}$$

- Limit on the power loss on the transmission line

The active power loss on the transmission lines have negative impacts on the power flow on these lines, which can affect the operational cost of generation and as well affect the scheduling of the renewable generation in the planning systems. Constraints (33) and (34) imposes that the real and reactive power loss on the line must be equals the net sum of inflowing and outflowing power on the line.

$$P_{loss} = g_l (V_\alpha^2 \text{+} V_\beta^2 - 2V_\alpha V_\beta \cos \theta_{\alpha\beta}) \forall l = 1, 2, ..., n_l \tag{33}$$

$$Q_{loss} = -b_{lo} (V_\alpha^2 \text{+} V_\beta^2) - b_l (V_\alpha^2 \text{+} V_\beta^2 - 2V_\alpha V_\beta \cos \theta_{\alpha\beta}) \forall l = 1, 2, ..., n_l \tag{34}$$

- Generation limits for conventional generating units

The real and reactive power generation limits for conventional generating units are given in constraints (36) and (37) respectively, and it imposes that the generating capacity must not be exceeded.

$$P_i^{min} \le P_i \le P_i^{max} \forall i = 1, 2, ..., n_i \tag{35}$$

$$Q_i^{min} \le Q_i \le Q_i^{max} \forall i = 1, 2, ..., n_i \tag{36}$$

- Generation limits for wind and solar generating units

The real and reactive power generation limits for offshore wind and solar farms are given in constraints (37) to (40) respectively, and it imposes that the optimal power from renewable energy generating units does not exceed its maximum limits.

$$0 \le P_w \le P_w^{max} \forall w = 1, 2, ..., n_w \tag{37}$$

$$Q_w^{min} \le Q_w \le Q_w^{max} \forall w = 1, 2, ..., n_w \tag{38}$$

$$0 \le P_s \le P_s^{max} \forall s = 1, 2, ..., n_s \tag{39}$$

$$Q_s^{min} \le Q_s \le Q_s^{max} \forall s = 1, 2, ..., n_s \tag{40}$$

- Limit on capacity of the transmission line

The power flow on the transmission branch circuit must not exceed its minimum and maximum operating capacity.

$$0 \le (F_l^{(outflow)})^2 \text{+} (Q_l^{(outflow)})^2 \le S_l^2 \forall l = 1, 2, ..., n_l \tag{41}$$

$$0 \le (F_l^{(inflow)})^2 + (Q_l^{(inflow)})^2 \le S_l^2 \forall l = 1, 2, ..., n_l \tag{42}$$

- Limit on magnitude and angle of bus voltage

Harmonics affect the bus voltages and sometimes can result in over and under voltage at the buses. The bus voltage must be kept in safety limits to avoid unnecessary stressing of electrical components. Constraints (43) and (44) ensure that the magnitudes and angles of operating voltage must be within the safe limit.

$$V_{min} \le V_b \le V_{max} \forall b = 1, 2, ..., n_b \tag{43}$$

$$-\pi \le \theta_b \le \pi \forall b = 1, 2, ..., n_b \tag{44}$$

C. Solution Methodology for Multi-Objective Optimization Problems.

The single solution that minimizes all the four objectives simultaneously does not exist because of the incomparability of the economic and technical objectives. From the literatures, there are many methods for converting multi-objective optimization problems into a single objective function serving as a condition for obtaining approximate Pareto optimal solutions. The methods of solution include weighted sum approach, ε-constraint approach [29] and augmented ε-constraint approach [30]. In this paper, weighted sum approach is employed for converting the economic and technical objectives into a single suitable solution because an approximate Pareto optimal solution is obtainable from this solution approach. In this solution approach, a weighting factor σ_i is designated to each objective and the composite objective function is minimized as [31]:

$$Min \sum_{i=1}^{n} \sigma_i F_i \tag{45}$$

subject to:

$$\sum_{i=1}^{n} \sigma_i = 1 \tag{46}$$

Therefore, it is often important to choose weighting factors based on the user preferences for various objectives to obtain a suitable single solution. In this work, equal preference is given to the four objectives since the aim is to simultaneously minimize the objectives and thus the weights $\sigma_1, \sigma_2, \sigma_3$ and σ_4 are equal and are nonnegative [32].

IV. NUMERICAL SIMULATION APPROACHS

In this section, two test bus systems which includes IEEE 6-bus and 24-bus test systems are used to validate the performance of the proposed mixed integer nonlinear programming (MINLP) model. Fig. 2 presents the flowchart for calculation of total costs, optimal marginal nodal prices, optimal generation scheduling and line flow considering harmonic losses. The flowchart can be summarized using the following steps:

- Step1: Modelling and harmonic simulation of IEEE bus system with offshore wind and solar farms using ETAP power station software (12.6.0).
- Step 2: Harmonic computation at the bus and on the lines using the equations (13) to (15).
- Step 3: Run optimal power flow on the IEEE bus system using MATLAB to obtain locational marginal pricing at each node.
- Step 4: Run regression analysis using Waikato Environment for Knowledge Analysis (WEKA) to obtain coefficient of locational marginal price as a function of harmonic power loss.
- Step 5: Solve the MINLP formulation using two different solvers SNOPT 7.2 and XA 16 in Advanced Interactive Multidimensional Modelling System Outer Approximation Algorithm (AOA). If the constraints are satisfied then obtain the costs, optimal nodal prices, optimal power generated by the conventional and renewable generating units
- Step 6: The gap between the two solvers approach zero, then finish. Otherwise go back to Step 5.
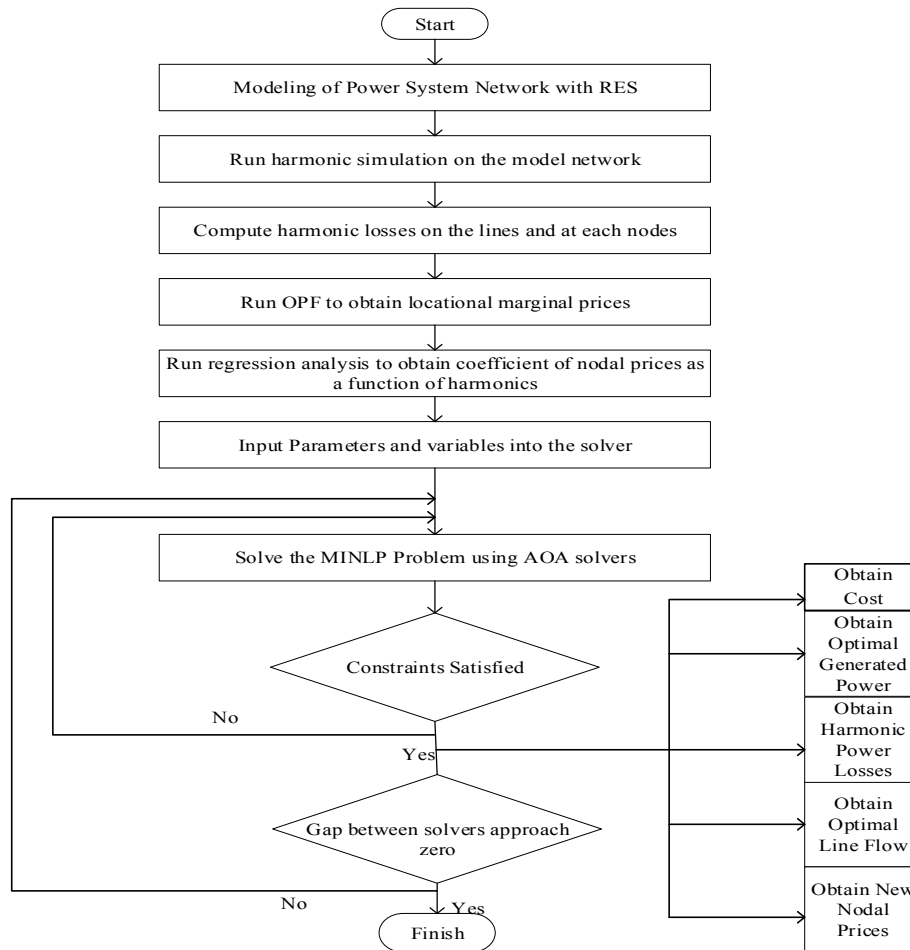
Figure 2: Flowchart for calculating economical costs, optimal generation scheduling and technical losses considering harmonics.

V. SIMULATION RESULTS

In this section, the proposed mixed integer nonlinear programming (MINLP) problem formulation is solved using Advanced Interactive Multidimensional Modelling System Outer Approximation Algorithm (AOA). The AOA transformed the mixed integer nonlinear programming (MINLP) problem into mixed integer linear programming (MILP) problem and nonlinear programming (NLP) problem using two different solvers SNOPT 7.2 and XA 16 respectively. Advanced Interactive Multidimensional Modelling System (AIMMS) is a unified combination of a modelling language, a graphical user interface and numerical solvers. AIMMS is a complete flexible modelling system designed for advances planning systems and large-scale optimization problems [33]- [35].

A. Results from IEEE Six Bus System

In this section, an IEEE six bus system is considered to demonstrate the performance of the proposed MINLP mathematical model. The single line diagram of this test bus system and the proposed sites of renewable energy sources and new transmission lines is shown in Fig. 3. The proposed renewable energy generators have been incorporated at bus 1, 2, 3 and 4. This test bus system consists of three generators, five loads, six transmission lines and six buses. The network data for cost coefficients and power rating of the thermal generators was obtained from [36]. In order to expand the network whilst considering the future demand forecast, there is an assumption that the load demand at each bus has been doubled. Hence, the system network loads for this case study is 1440 MW.
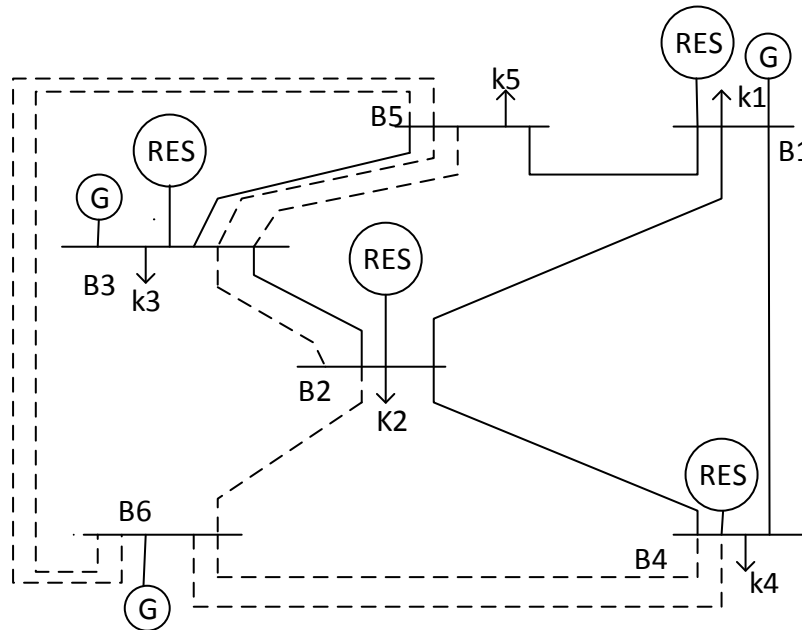
Figure 3: IEEE Garver Six-Bus System with Proposed Renewable Energy Sources.

Table 1 shows the results obtained from harmonic analysis simulation at each bus on the six-bus system with consideration to the proposed renewable energy generators. The presence of

harmonics on the network is as a result of the nonlinear behavior of the power electronic components of the renewable energy generators on the network. The optimized results for power output from the conventional generating units and renewable energy generating units are shown in Tables 2 and 3 respectively.

Table 1: Voltage Total Harmonic Distortion at Six Bus System with Renewable Energy Sources.

Buses	Voltage (kV)	THD_V (%)	IEEE Limit (%)	Conclusion
1	400	6.88	2.5	Exceeded
2	400	8.15	2.5	Exceeded
3	400	7.09	2.5	Exceeded
4	400	8.72	2.5	Exceeded
5	400	7.65	2.5	Exceeded
6	400	10.82	2.5	Exceeded

Table 2: Optimal Power Output from Conventional Generators of a Six Bus System.

Buses	Installed Capacity (MW)	Optimal Output (MW)
1	160	158.7
3	360	82.8
6	600	176.9

Table 3: Optimal Power Output from Offshore Wind and Solar PV Farms of Six Bus System

Buses	Optimal Solar Power (MW)	Optimal Wind Power (MW)
1	13	165
2	15.5	275
3	18	325
4	13	185

Table 4 shows the calculated nodal prices at each bus of the network with and without the incorporation of RES. The obtained results from the proposed method show three different

marginal nodal prices which includes the nodal price without RES (N_p), the nodal price with incorporation of RES but without consideration to harmonics from RES ($N_{RES,p}$) and the nodal price with RES and harmonics ($N_{RES,p}^h$). Also, the nodal marginal price coefficients obtained from the regression analysis and the minimized harmonic power losses obtained at the buses are presented in Table 4. Table 5 gives the detail of the optimized outflowing and inflowing power into the existing and prospective transmission lines. A total of eight additional transmission lines are required to be added to the system network. Table 5 also shows the active power and harmonic power losses on the existing and prospective transmission lines. Table 6 provides a numerical results comparison between when the system network is without and with renewable energy sources. From the obtained results, it shows that the incorporation of renewable energy generating units contributes to presence of harmonic distortion on the network which result into increase in the nodal marginal prices and losses on the system network.

Table 4: Nodal Marginal Prices with RES ($N_{RES,p}$), RES and harmonics ($N_{RES,p}^h$) and without RES (N_p) of a Six Bus System.

Buses	x_b	y_b	z_b	N_p (MW)	$N_{RES,p}$ (MW)	$N_{RES,p}^h$ (MW)	Harmonic Power Loss (MW)
1	0.001	-0.0042	15.9101	36.47	15.89	24.01103	0.202
2	0.0001	-0.0025	16.5895	37.5	16.57	17.55689	0.281
3	0.0001	-0.0005	15.5781	34.98	15.56	18.62111	0.367
4	0.0001	-0.0009	17.6887	40.13	17.67	28.79575	0.524
5	0.0001	-0.0016	18.333	40.35	18.31	22.38762	0.732
6	0.0001	-0.0005	17.217	39.3	17.2	35.37885	0.916
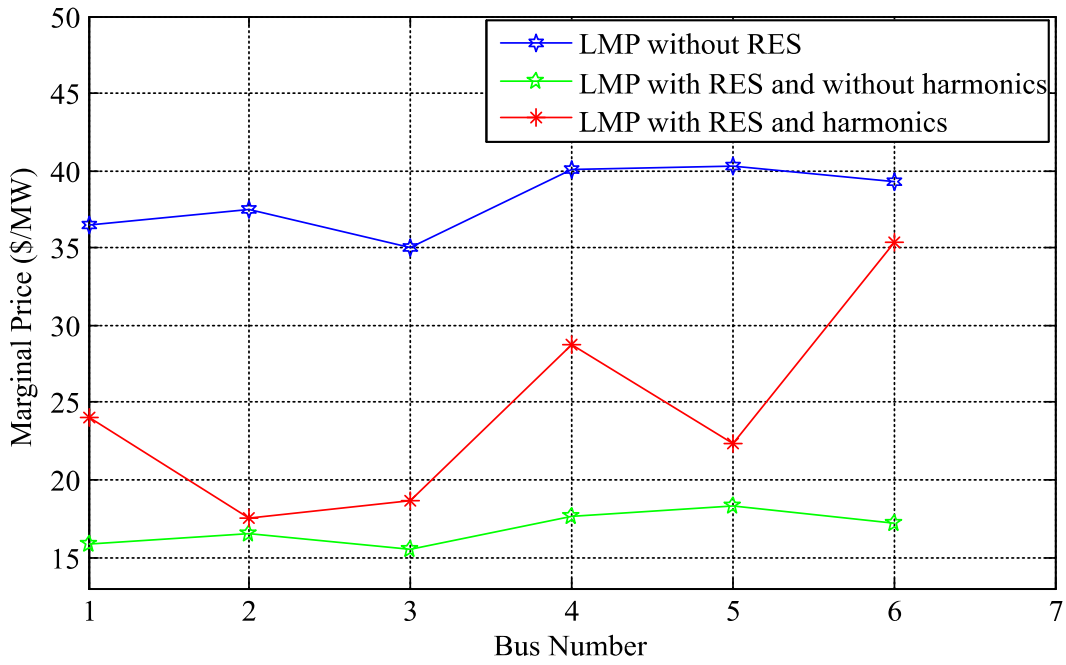
Figure 4: Variation in nodal marginal price with and without harmonics in 6-bus system.
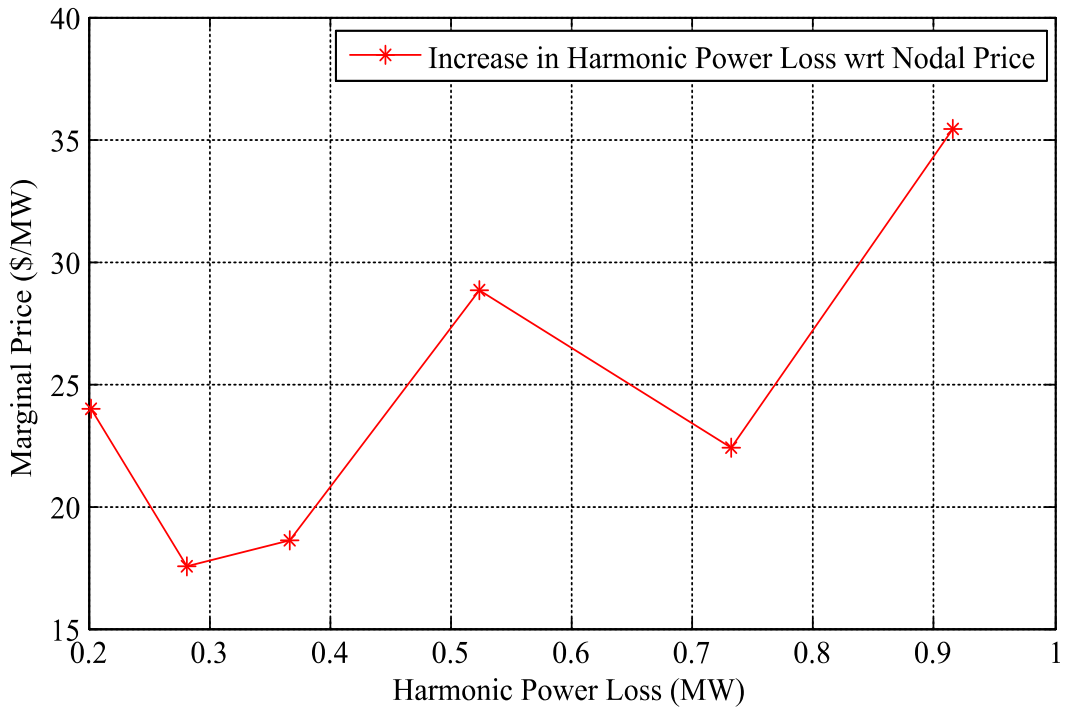
Figure 5: Variation of harmonic power loss with respect to optimal nodal price in 6-bus system.

Table 5: Harmonic and Power Losses on Transmission Lines of Six Bus System.

S/N	Between Buses	$F_l^{(outflow)}$ (MW)	$F_l^{(inflow)}$ (MW)	Line Losses (MW)	Harmonic Power Loss (MW)
1	1-2	41.31083	-40.5646	0.74623	0.001371
2	1-4	27.48503	-26.9885	0.49648	0.001346
3	1-5	108.6348	-106.018	2.61678	0.035539
4	2-3	53.2796	-52.3777	0.90189	0.164487
5	2-3	53.2796	-52.3777	0.90189	0.164487
6	2-6	82.23738	-80.5935	1.64388	0.081652
7	3-5	82.23738	-80.5935	1.64388	0.081652
8	3-5	82.23738	-80.5935	1.64388	0.081652
9	3-5	37.48126	-37.0116	0.46964	1.020434
10	4-6	37.48126	-37.0116	0.46964	0.80941
11	4-6	37.48126	-37.0116	0.46964	0.80941
12	5-6	27.0103	-26.509	0.50126	0.887916
13	5-6	27.0103	-26.509	0.50126	0.887916
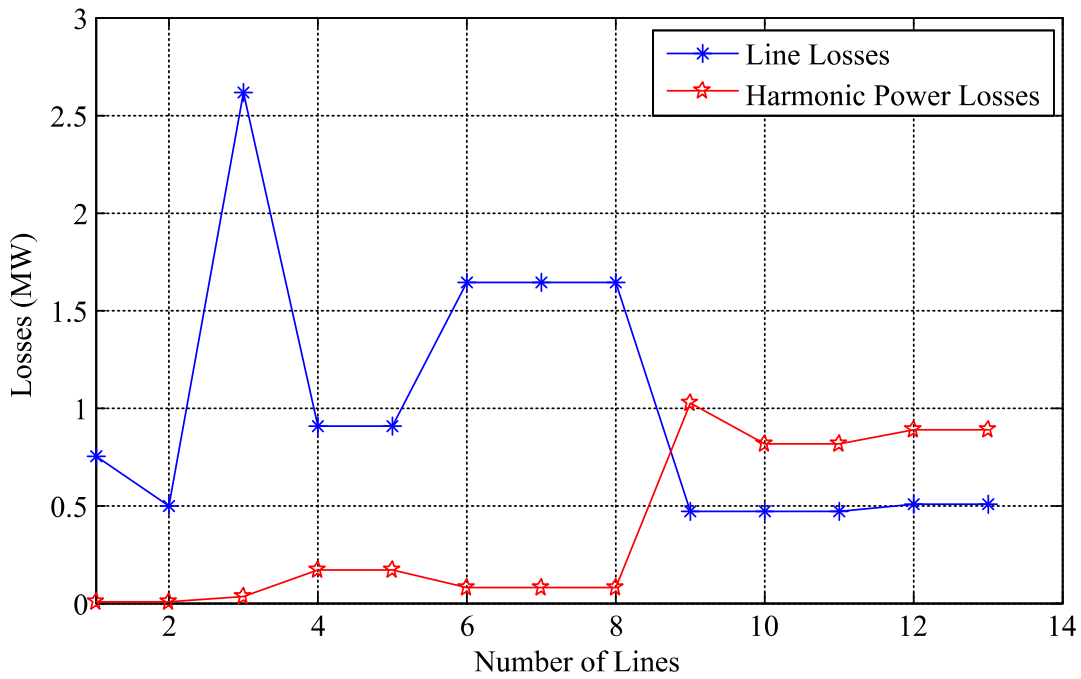
Figure 6: Transmission line active power loss and harmonic power loss in 6-bus system.
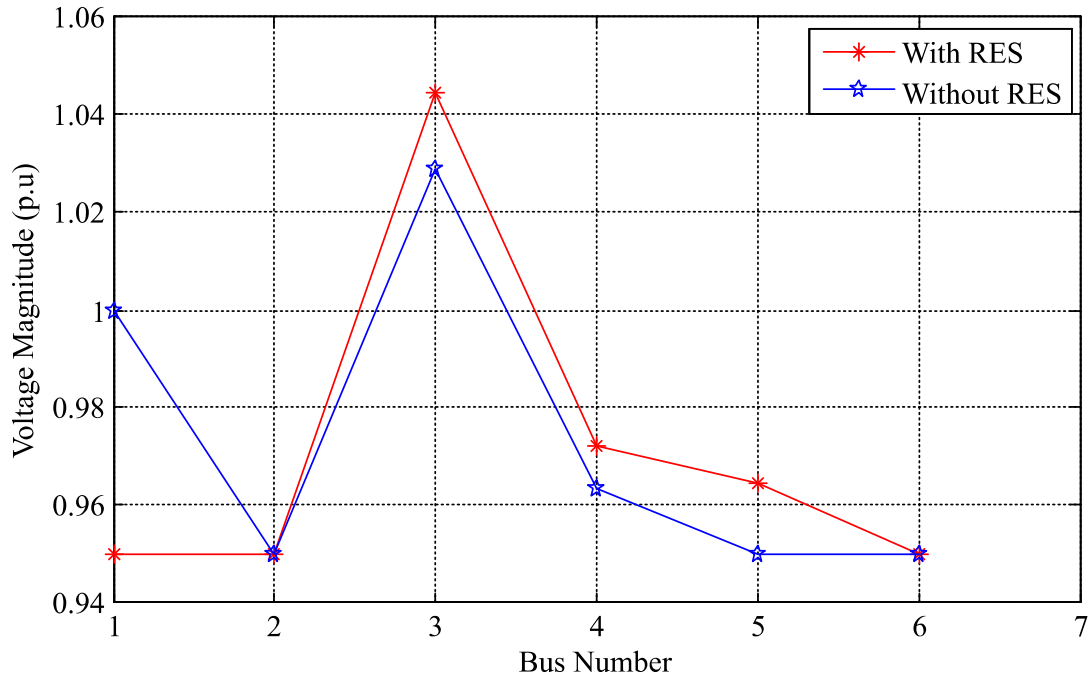
Figure 7: Variation in magnitudes of bus voltage in 6-bus system.

Table 6: Final parameters of the IEEE Six Bus System without and with RES

	Without RES	With RES
Cost ($\times 10^6$\$)	199.4	134.4
Active power losses (MW)	10.85	13.01
Nodal Price (\$/MW)	228.73	146.76
Harmonic Loss (MW)	-	5.03
New Lines	8	7

B. Results from IEEE 24 Bus System

In this section, the performance of the proposed model is validated on a larger bus system of IEEE 24 bus system to check the efficiency of the model. The case study consists of thirty-three generators, thirty-eight transmission lines, seventeen loads and twenty-four buses. The network is divided into two parts, the first part has a 138 kV network with maximum generation capacity of 340 MW and available loads of 1332 MW, while the second part has a 230 kV with maximum generation capacity of 1436 MW and the load demand of 1518 MW. The network data for this test bus system can be found in [36]. In order to allow investment decisions in both generation

22

and transmission expansion planning due to load forecast on the network, we assumed that the load on the network is doubled and the transmission capacities are reduced by three quarters.

Table 7 presents the results from harmonic analysis on the 24-bus system considering the incorporation of the proposed renewable energy generators. The nonlinearity of the renewable energy generators and the transmitting components give rise to harmonics exceeding their standard limit. Tables 8 and 9 show the optimized power output from the conventional and renewable energy generating units on the 24-bus system respectively. Table 10 presents result of the calculated nodal marginal price as a function of harmonics from the proposed model alongside with nodal price without harmonics when the RES is incorporated into the power system. The nodal price function coefficients and the minimized harmonic power losses at the buses are presented in Table 10.

Table 7: Voltage Total Harmonic Distortion at 24 Bus System with Renewable Energy Sources.

Buses	Voltage (kV)	THD_V (%)	IEEE Limit (%)	Conclusion
1	138	60.14	2.5	Exceeded
2	138	58.11	2.5	Exceeded
3	138	54.11	2.5	Exceeded
4	138	55.68	2.5	Exceeded
5	138	62.66	2.5	Exceeded
6	138	77.98	2.5	Exceeded
7	138	52.02	2.5	Exceeded
8	138	59.85	2.5	Exceeded
9	138	47.11	2.5	Exceeded
10	138	66.52	2.5	Exceeded
11	230	34.28	2.5	Exceeded
12	230	29.27	2.5	Exceeded
13	230	23.18	2.5	Exceeded
14	230	27.42	2.5	Exceeded
15	230	22.96	2.5	Exceeded
16	230	23.22	2.5	Exceeded
17	230	18.29	2.5	Exceeded
18	230	16.57	2.5	Exceeded
19	230	27.99	2.5	Exceeded
20	230	22.98	2.5	Exceeded
21	230	17.07	2.5	Exceeded
22	230	13.96	2.5	Exceeded
23	230	20.77	2.5	Exceeded
24	230	44.66	2.5	Exceeded

Table 8: Optimal Power Output from Conventional Generators of a 24 Bus System.

Buses	Installed Capacity (MW)	Optimal Output (MW)
1	192	155
2	192	180
7	300	300
13	591	286.22
15	215	165
16	155	155
18	400	400
21	400	375.44
22	300	237.36
23	660	300

Table 9: Optimal Power Output from Offshore Wind and Solar PV Farms of 24 Bus System

Buses	Optimal Solar Power (MW)	Optimal Wind Power (MW)
1	50	238.054
3	70	100
6	85	173.91
8	90	175.75
10	100	279.47
15	75	275
18	85.49	235
19	85	338.85
24	71	130

Table 10: Nodal Marginal Prices with RES ($N_{RES,p}$), RES and harmonics ($N_{RES,p}^h$) and without RES (N_p) of a 24-Bus System.

Buses	x_b	y_b	z_b	N_p ($/MW)	$N_{RES,p}$ ($/MW)	$N_{RES,p}^h$ ($/MW)	Harmonic Power Loss (MW)
1	-0.0002	0.077	16.718	49.59	16.72	23.82001	1.05792
2	-0.0002	0.08932	17.538	49.61	17.55	26.23867	1.435844
3	0.00225	-0.138	16.409	49.68	16.31	26.98961	1.531784
4	-0.57	1.612	18.369	51.12	18.38	18.98608	0.023748
5	-0.24	1.95	17.408	50.85	17.51	19.05184	0.071623
6	0.0244	-0.028	17.652	51.82	17.65	22.22603	0.142683
7	-0.00324	0.363	17.647	51.07	17.64	41.13542	2.849308
8	0.00247	-0.1901	17.074	52.43	17.09	33.35222	1.774068
9	0.002382	-0.1612	17.683	50.4	17.57	33.51475	1.793146
10	-0.004	1.188	17.073	50.66	17.26	29.61986	1.757137
11	0.0032	-0.196	17.121	50.27	17.29	21.59573	0.789627
12	0.01197	-0.499	17.416	50.17	17.19	22.19561	0.8492
13	-0.838	2.5121	17.5	49.71	17.22	19.15458	0.019557
14	1.307	-0.772	17.82	49.45	17.47	17.62553	0.01905
15	0.0616	-0.145	17.031	47.64	16.96	21.11213	0.69001
16	0.02733	-0.041	17.047	47.81	17	20.3197	0.119677
17	0.0545	-0.2525	17.387	46.87	16.85	17.79799	0.042597
18	0.1404	-0.1587	16.872	46.58	16.83	22.16187	0.22725
19	-0.0449	0.9899	16.966	48.05	16.89	23.85207	0.93851
20	0.0119	-0.0905	16.709	47.83	16.82	18.86467	0.163523
21	0.9078	-2.868	17.71	46.41	16.69	16.48826	0.022145
22	0.0077	-1.4843	16.583	45.24	16.27	17.09256	0.0986
23	0.2133	-0.59741	16.842	47.56	16.67	22.80846	0.68322
24	-0.00011	0.1424	16.418	49	16.43	23.54229	1.050888
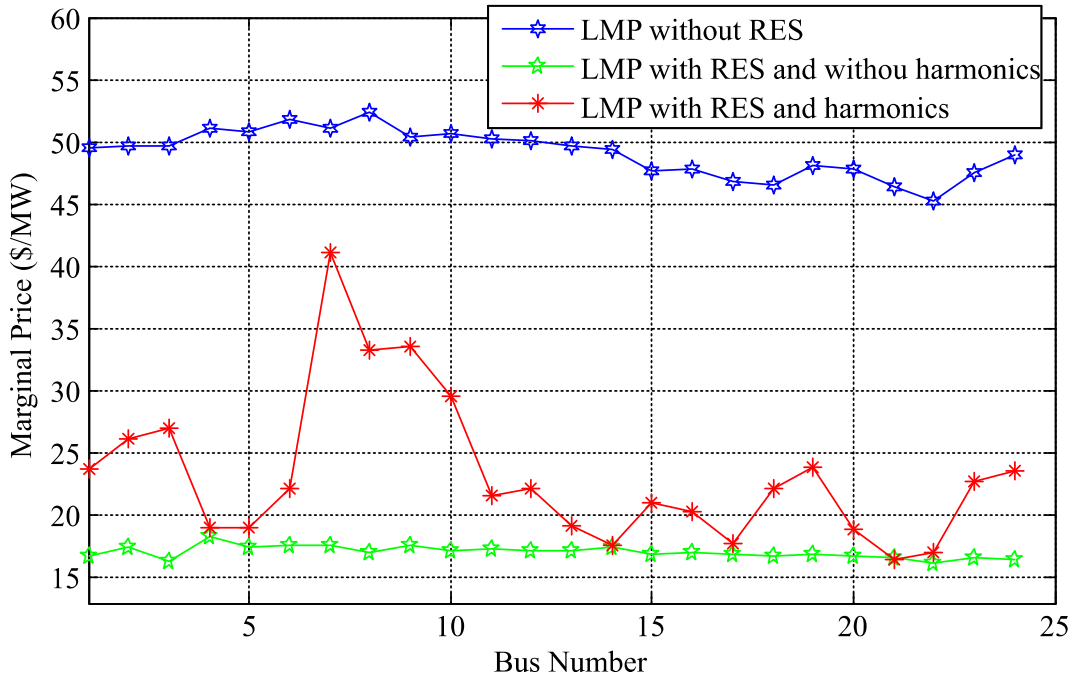
Figure 8: Variation in nodal marginal price with and without harmonics in 24-bus system.

Table 11 shows the inflow and outflow power on the existing and prospective transmission lines. From the obtained results, a total of twelve prospective lines are required to be added to the network. The active power and harmonic power losses on the existing and prospective transmission lines are also presented in Fig. 9. Table 12 gives numerical results showing comparison on the test system network without and with the incorporation of renewable energy generating units. The result shows that the introduction of the renewable energy generating units into the network results into increase in the total losses on the network.

Table 11: Harmonic and Power Losses on Transmission Lines of a 24 Bus System.

Lines	Between Buses	$F_l^{(outflow)}$ (MW)	$F_l^{(inflow)}$ (MW)	Line Losses (MW)	Harmonic Power Loss (MW)
1	1-2	47.88674	-45.6616	2.22514	1.75004
2	1-3	3.756093	-3.62776	0.12833	0.3085
3	1-5	74.25694	-73.8313	0.42561	0.09496
4	2-4	48.51397	-48.1306	0.38333	0.76739
5	2-6	2.207186	-1.95085	0.25634	0.13945
6	3-9	24.19682	-23.6946	0.5022	0.13528
7	3-24	297.3768	-291.155	6.22143	0.50044
8	4-9	41.35066	-40.9661	0.38456	0.0673
9	5-10	5.279755	-5.20956	0.0702	0.07213
10	6-10	5.884062	-5.1	0.78406	0.50623

26

| 11	7-8	39.78379	-39.2744	0.50939	1.3937
12	8-9	7.177423	-6.84286	0.33456	0.13409
14	9-11	52.32119	-51.5943	0.72691	1.69283
15	9-12	125.2687	-120.357	4.91164	0.52919
16	10-11	28.92975	-28.7552	0.17451	4.39899
17	10-12	95.4622	-92.2775	3.18468	5.28148
18	11-13	92.26683	-90.7298	1.53704	0.35993
20	12-13	49.05736	-48.4265	0.6309	0.47883
21	12-23	199.3287	-190.218	9.11074	0.13157
22	13-23	166.478	-158.01	8.46835	0.14208
23	14-16	227.1257	-221.78	5.346	0.41538
24	15-16	130.1462	-125.738	4.40776	1.38568
25	15-21	148.5703	-144.477	4.09315	0.25128
26	15-21	148.5703	-144.477	4.09315	0.25128
27	15-24	39.28753	-34.1337	5.15383	0.29196
28	16-17	130.3374	-126.021	4.31694	0.61346
29	16-19	45.42122	-44.0572	1.36402	0.84826
30	17-18	20.73724	-20.2881	0.44912	1.39535
31	17-22	112.2627	-108.931	3.33185	0.00408
32	18-21	40.40458	-40.3138	0.09079	0.63809
33	18-21	40.40458	-40.3138	0.09079	0.63809
34	19-20	29.53297	-29.3666	0.16633	0.20534
35	19-20	29.53297	-29.3666	0.16633	0.20534
36	20-23	104.1022	-100.856	3.24652	0.32282
37	20-23	104.1022	-100.856	3.24652	0.32282
38	20-23	64.39553	-60.3155	4.08	1.750043
39	1-2	68.81393	-66.075	2.73895	1.75004
40	1-5	74.25337	-73.8296	0.42376	0.09496
41	2-4	48.52459	-48.1379	0.38671	0.76739
42	3-9	24.19682	-23.6946	0.5022	0.13528
43	8-9	7.203183	-6.87085	0.33233	0.13409
45	12-13	49.05736	-48.4265	0.6309	0.47883
46	15-16	130.1462	-125.738	4.40776	1.38568
47	17-18	20.73724	-20.2881	0.44912	1.39535
48	18-21	40.40458	-40.3138	0.09079	0.63809
49	18-21	40.40458	-40.3138	0.09079	0.63809
50	22-23	123.3418	-120.667	2.67444	0.07442
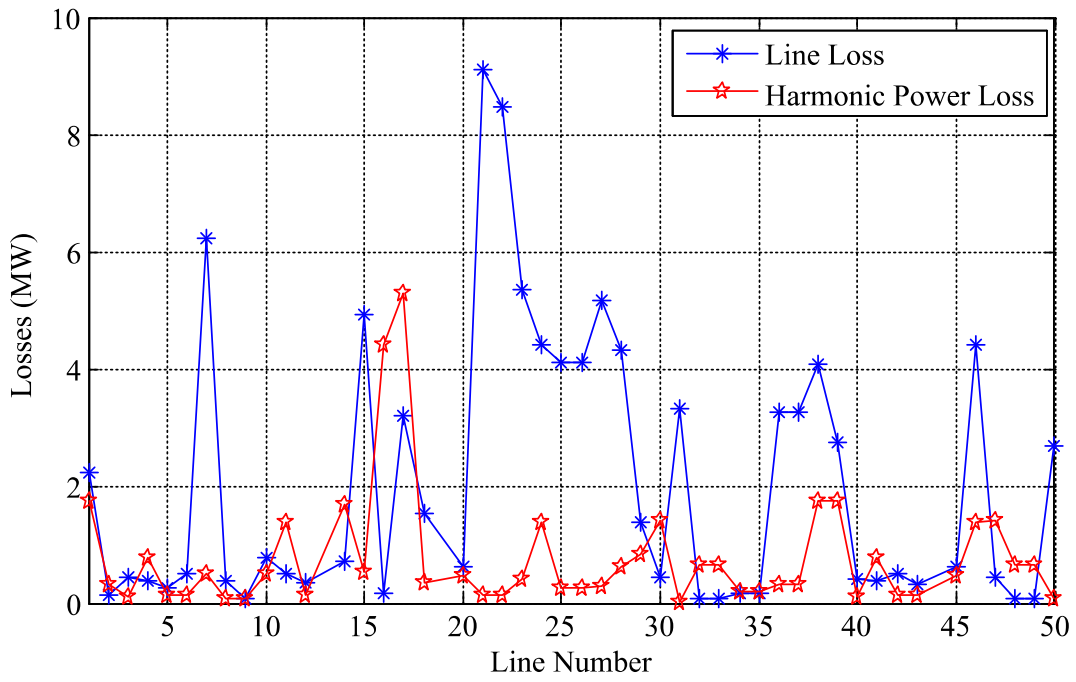
Figure 9: Transmission line active power loss and harmonic power loss in the 24-bus system.
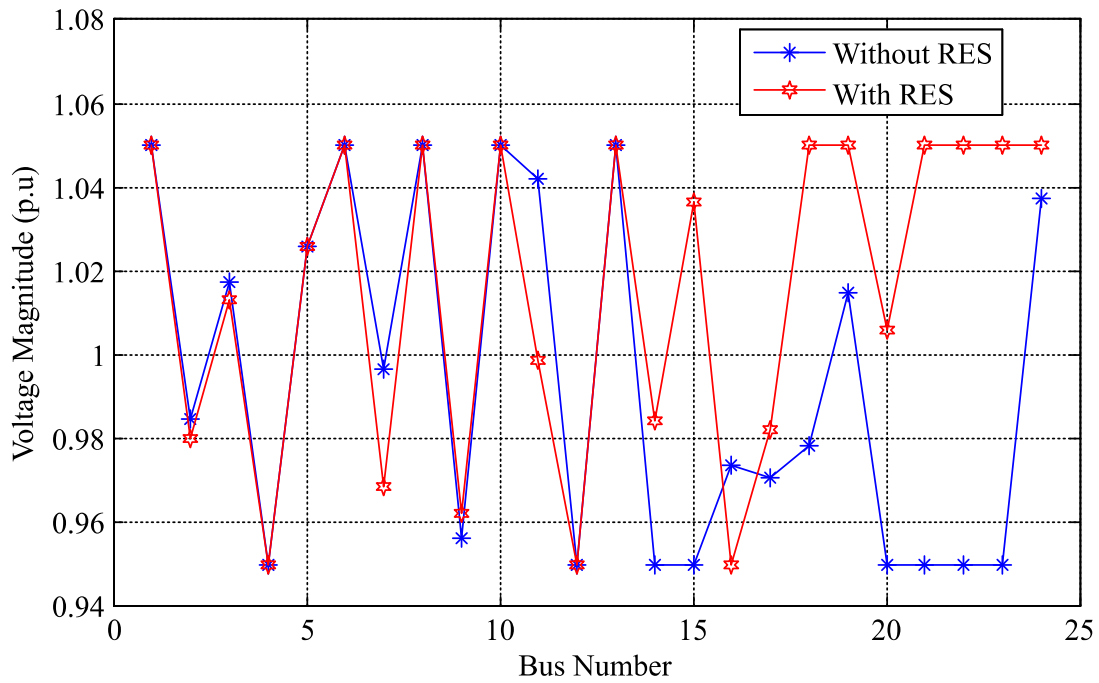

Figure 10: Variation in magnitudes of bus voltage in 24-bus system.

Table 12: Characteristics of IEEE 24 Bus System without and with RES.

	Without RES	With RES
Cost (10^6\$)	840.88	735.59
Active power losses (MW)	72.96	97.34
Nodal Price (\$/MW)	1179.82	559.55
Harmonic Loss (MW)	-	35.92
New Lines	14	12

VI. DISCUSSION OF RESULTS

In this section, the presented simulated results from the two case studies will be discussed and analyzed. The optimization results obtained can be discussed along two lines, which is comparison of the system network without and with the incorporation of Renewable Energy Sources. In the discussion, emphasis would be on the economic and technical power system parameters such as the total cost (\$), nodal marginal price (\$/MW), active power loss (MW) and harmonic power loss (MW).

Results obtained from Tables 1 and 7 show the harmonic characteristics of the voltage total harmonic distortions obtained in 6-bus and 24-bus systems respectively. It can be inferred from the results that the harmonic contents are relatively higher and exceeded the recommended IEEE standard limit at all buses. It is obvious that the buses far from the RES experience more Voltage Total Harmonic Distortion (VTHD). As shown in Table 7, the VTHD decreases with increase in bus voltage, the reason is that the source impedance of the far end buses is much smaller as the path length of the transmission lines impedance increases and thus the voltage harmonic distortion is magnified at the bus. In order to expand the network for future load forecast, the conventional generating units are supported by the renewable energy sources since the conventional generators cannot meet the demand. The simulated results in Tables 2 and 3 shows that the optimal power output in a 6-bus system by conventional generators to be 450.5 MW and by the renewable energy generating units is 1009.5 MW respectively, while Tables 8 and 9 gives details of the optimized power output in 24-bus system from conventional generators to be 2554.02 MW and from the renewable energy generating units to be 2657.53 MW.

As seen in Figs. 4 and 8, the changes in locational marginal prices with RES ($N_{RES,p}$), RES and harmonics ($N_{RES,p}^h$) and without RES (N_p) in 6-bus and 24-bus systems respectively. $N_{RES,p}$ does not practically interpret the marginal nodal prices at the bus, because it is evidently clearly as shown in Tables 1 and 7, that RES contributes to harmonic emissions on the network. $N_{RES,p}$ does not capture the harmonic emissions as a result of RES at the buses, which renders it

29

inappropriate method of obtaining LMP on the network with RES. Figs. 4 and 8 give the graphical representation of the results obtained from the proposed method ($N^h_{RES,p}$) of calculating marginal nodal prices with consideration to harmonic emission from RES on the power system network. It is obvious that the proposed method ($N^h_{RES,p}$) gives lower marginal nodal prices than N_p. These values ($N^h_{RES,p}$) are relatively higher than $N_{RES,p}$ because they consider the harmonic emissions present in RES. Thus, this implies that the cost of generating an extra MW of power at each bus depends on the magnitude of harmonic emissions present at that point. Fig. 5 depicts the results of harmonic power loss variation with nodal marginal price. It is obvious from the obtained results that an increase in harmonic power loss causes increase in the optimal nodal marginal price which influence the costs of generation of extra MW of power at each bus.

As it is widely known that harmonics can't be completely eliminated but can only be reduced [7], Figs. 6 and 9 show the minimized active power losses and harmonic power losses in 6-bus system to be 13.01 MW and 5.03 MW respectively, while that of 24-bus system are 97.34 MW and 35.92 MW respectively. It is obvious from the obtained results that the power system experiences a minimal 0.5% and 1.35% losses from RES to harmonics in 6-bus and 24-bus systems respectively. Figs. 7 and 10 show the variations in voltage profile with and without RES in 6-bus and 24-bus test systems. It can be seen that the voltage profile of the system is improved with the incorporation of RES on the power system network. The presented analysis based on the comparison of the power system without and with the incorporation of RES for 6-bus and 24-bus systems as shown in Tables 6 and 12 respectively, shows that the proposed model improves costs reduction from $199.4×10^6$ to $134.4×10^6$ in the 6-bus system and $849.88×10^6$ to $735.559×10^6$ in 24-bus system. Also, the integration of RES into the power system significantly reduced locational marginal prices from $228.73/MW to $146.76/MW in 6-bus system and $1179.82/MW to $559.55/MW and likewise reduced the number of additional transmission lines required to be added to the system from eight to seven lines and fourteen to twelve lines in the 6-bus and 24-bus systems respectively.

VII. CONCLUSIONS

This paper presents a multi-objective AC optimization model that is proposed to minimize the total costs, power loss and harmonics loss in a grid whilst considering its impact on the nodal marginal prices and expansion planning of the power system. The harmonics from the renewable energy generating units and transmitting medium are analyzed using ETAP software. The efficiency of the proposed model was validated using IEEE 6-bus and 24-bus test systems and the following conclusions can be drawn from the numerical simulation results.

- The incorporation of RES in the power system improves the voltage profile of the system network which demonstrate the importance of RES in enhancing the voltage profile on the system network.
- The higher the number of buses with RES, the more the harmonic distortions on the network and the greater the harmonic power losses. The proposed model causes

improvement in cost reduction, nodal marginal price reduction and minimal additional lines when RES is introduced into the power system.

The proposed model serves as an accurate and effective methodology for calculating nodal marginal price with consideration to harmonic emissions from RES integration. This will serve as a better solution for real life expansion planning problems. In the future, we will consider the impacts of the stochastic nature of harmonics, wind power and the load on the expansion planning problem.

Acknowledgement

References

[1]   M. Parker, S. Finney, and D. Holliday, Energy Procedia, **142**, 2195 (2017).

[2]   M. Ahmed, S. Mekhilef, M. Mubin, and M. Aamir, Renew. Sustain. Energy Rev., **82**, 2235, (2018).

[3]   IEEE Standard Definitions for the Measurement of Electric Power Quantities Under Sinusoidal, Non-sinusoidal, Balanced, or Unbalanced Conditions, IEEE Std 1459-2010 (Revision of IEEE Std 1459-2000), 1 (2010).

[4]   S. L. Gbadamosi and A. O. Melodi, Int. Inst. Sci. Technol. Educ., **3 (**10), 8, (2013).

[5]   V. Bečirović, I. Pavić, and B. Filipović-Grčić, Electr. Power Syst. Res., **154**, 515, (2018).

[6]   R. Arghandeh, A. Onen, J. Jung, and R. P. Broadwater, Electr. Power Syst. Res., **105**, 124, (2013).

[7]   S. L. Gbadamosi and A. Melodi, Adv. Sci. Technol. Res. J., **9**, 1, (2015).

[8]   M. Kumawat, N. Gupta, N. Jain, and R. C. Bansal, Swarm Evol. Comput., **39**, 99, (2018).

[9]   S. Nojeng, M. Y. Hassan, and D. M. Said, J. Electr. Eng. Technol.,**9**, 742, (2014).

[10]   J. J. R.-M. S. García-Martínez, E. Espinosa-Juárez, 2012 9th Int. Conf. Electr. Eng. Comput. Sci. Autom. Control, **443**, 1, (2012).

[11]   L. Sainz, J. J. Mesas, R. Teodorescu, and P. Rodriguez, IEEE Trans. Energy Convers., **25**, 1071, (2010).

[12]   R. King and J. B. Ekanayake, IEEE PES Gen. Meet. PES 2010, 1, (2010).

[13]   P. P. Biswas, P. N. Suganthan, and G. A. J. Amaratunga, Appl. Soft Comput. J., **61**, 486, (2017).

[14] Y. Kabalci, S. Kockanat, and E. Kabalci, Electr. Power Syst. Res., **154**, 160, (2018).

[15] X. Li, P. Duan, I. Kockar, and K. L. Lo, Universities Power Engineering Conference (UPEC), 2012 47th International, 1, (2012).

[16] A. Arabali, M. Ghofrani, M. Etezadi-Amoli, M. S. Fadali, and M. Moeini-Aghtaie, IEEE Trans. POWER Syst., **29,** 3003, (2014).

[17] E. Azad-farsani, S. M. M. Agah, H. Askarian-abyaneh, M. Abedi, and S. H. Hosseinian, Energy, **107**, 396, (2016).

[18] K. R. Devabalaji, A. M. Imran, T. Yuvaraj, and K. Ravi, Power Loss Minimization in Radial Distribution System, vol. 79. Elsevier B.V., 2015.

[19] E. Azad-Farsani, Energy, **140**, 1, (2017).

[20] F. Kunz, K. Neuhoff, and J. Rosellón, Energy Econ., **60**, 176, (2016).

[21] M. Liu, F. L. Quilumba, and W. J. Lee, IEEE Trans. Ind. Appl., **51**, 1970, (2015).

[22] J. M. Morales and J. Pérez-ruiz, IEEE Trans. Power Syst., **26**, 1, (2011).

[23] J. A. Momoh, Y. Xia, and G. D. Boswell, IEEE Power Energy Soc. Gen. Meet. Convers. Deliv. Electr. Energy 21st Century, PES, (2008).

[24] S. Gu Kim, Inst. Electr. Electron. Eng., 677, (2007).

[25] P. M. Sotkiewicz and J. M. Vignolo, IEEE Trans. Power Syst., **21**, 1, (2005).

[26] R. Torquato, W. Freitas, G. R. T. Hax, A. R. Donadon, and R. Moya, Proc. Int. Conf. Harmon. Qual. Power, ICHQP, 623, (2016).

[27] K. Yang, M. H. J. Bollen, H. Amaris, and C. Alvarez, Electr. Power Syst. Res., **141**, 84, (2016).

[28] Z. Ma, G. You, and Z. Xu, POWERCON 2014 - 2014 Int. Conf. Power Syst. Technol. Towar. Green, Effic. Smart Power Syst. Proc., 2332, (2014).

[29] F. Fathipour and M. Saidi-mehrabad, J. Renew. Sustain. Energy, **10**, 1, (2018).

[30] J. Aghaei, M. A. Akbari, A. Roosta, M. Gitizadeh, and T. Niknam, IET Gener. Transm. Distrib., **6**, 773, (2012).

[31] R. T. Marler and J. S. Arora, Struct. Multidiscip. Optim., **41**, 853, (2010).

[32] N. I. Nwulu and X. Xia, Renew. Energy, **101**, 16, (2017).

[33] S. Lee, H. Kim, and W. Kim, J. Electr. Eng. Technol., **12**, 2187, (2017).

[34] M. Hunting, Paragon Decis. Technol, 1, (2011).

[35] U. Damisa, N. I. Nwulu, and Y. Sun, IET Renew. Power Gener., **12**, 910, (2018).

[36] H. Zhang, Arizona State University Thesis, 2013.

Offshore Wind Farm

HVDC Link

PCC

Grid

AC
DC

DC
AC

Solar PV Farm i_s^h

i_τ^h

```
                              ┌─────────┐
                              │  Start  │
                              └─────────┘
                                   │
                                   ▼
        ┌──────────────────────────────────────────────────┐
        │      Modeling of Power System Network with RES     │
        └──────────────────────────────────────────────────┘
                                   │
                                   ▼
        ┌──────────────────────────────────────────────────┐
        │       Run harmonic simulation on the model network │
        └──────────────────────────────────────────────────┘
                                   │
                                   ▼
        ┌──────────────────────────────────────────────────┐
        │   Compute harmonic losses on the lines and at each nodes │
        └──────────────────────────────────────────────────┘
                                   │
                                   ▼
        ┌──────────────────────────────────────────────────┐
        │        Run OPF to obtain locational marginal prices │
        └──────────────────────────────────────────────────┘
                                   │
                                   ▼
        ┌──────────────────────────────────────────────────┐
        │  Run regression analysis to obtain coefficient of nodal prices as │
        │                 a function of harmonics            │
        └──────────────────────────────────────────────────┘
                                   │
                                   ▼
        ┌──────────────────────────────────────────────────┐
        │       Input Parameters and variables into the solver │
        └──────────────────────────────────────────────────┘
                                   │
                                   ▼
        ┌──────────────────────────────────────────────────┐
        │        Solve the MINLP Problem using AOA solvers   │
        └──────────────────────────────────────────────────┘
```

Start

Modeling of Power System Network with RES

Run harmonic simulation on the model network

Compute harmonic losses on the lines and at each nodes

Run OPF to obtain locational marginal prices

Run regression analysis to obtain coefficient of nodal prices as a function of harmonics

Input Parameters and variables into the solver

Solve the MINLP Problem using AOA solvers

Constraints Satisfied

No

Yes

Gap between solvers approach zero

No

Yes

Finish

Obtain Cost

Obtain Optimal Generated Power

Obtain Harmonic Power Losses

Obtain Optimal Line Flow

Obtain New Nodal Prices

Legend: Increase in Harmonic Power Loss wrt Nodal Price

X-axis: Harmonic Power Loss (MW)

Y-axis: Marginal Price ($/MW)